

# Erosion–corrosion of stainless steel pipes under two-phase flow with steam quality 26%

Mitsutaka H. Koike \*

*Safety Promotion Project, Japan Nuclear Cycle Development Institute, 4-49 Muramatsu, Tokai, Naka, Ibaraki 319-1184, Japan*

Received 31 August 2004; accepted 18 March 2005

## Abstract

High-speed, two-phase, water vapour flows in the outlet pipes of power reactors.

Erosion–corrosion experiments of stainless steel pipes were performed by the use of a component test loop, in which high-temperature, pressurized water vapour is circulated. Small pipe specimens were fixed in the pipes, and erosion–corrosion testing was performed under a two-phase flow of 28.8 t/h with steam quality 26%. Erosion–corrosion losses were very small and almost constant for steam phase velocities of 14–53 m/s.

© 2005 Elsevier B.V. All rights reserved.

## 1. Introduction

Japan Nuclear Cycle Development Institute has developed the ATR-Fugen, a 165 MWe prototype boiling-light-water-cooled heavy-water-moderated pressure-tube-type reactor of Japan, which has operated satisfactorily since the start of commercial operation in March 1979. The ATR is a unique reactor designed mainly to use plutonium–uranium mixed oxide fuels.

A 600 MWe ATR Demonstration Plant has been designed on the basis of the experience of the Fugen. The demonstration reactor has 648 outlet pipes in which high-speed two-phase water (ca. 280 °C, 7 MPa) flows from pressure tube to steam drum. The outlet pipes are made of type 316 stainless steel and about 75 mm in size. The design value of average steam phase velocity of two-phase flow in the outlet pipes is about 14 m/s,

and the maximum velocity is about 20 m/s. Design values of the average and maximum steam qualities in the outlet pipes are about 16% and 30%, respectively. It must be certified that outlet pipes are enduring under these conditions throughout the life of the reactor operation.

There have been few erosion experiments and theories under water–vapour two-phase flow for steam qualities of 10–30% (annular mist flow type). Therefore, erosion–corrosion experiments of type 316L stainless steel are conducted in this work under water–vapour high-speed two-phase flow conditions, with parameters of flow speed by the use of component test loop (CTL). The CTL is a full-scale test facility simulating the primary cooling circuit of the ATR in terms of coolant temperature and pressure.

Ito [1] performed erosion–corrosion experiments of stainless steel under high-temperature water with velocities of 1–12 m/s. Okada [2] performed cavitation–erosion tests by water for carbon steels. Investigations were performed by Palomero [3] on erosion–corrosion of steam generator tubes of a nuclear power station.

\* Tel.: +81 29 282 1122; fax: +81 29 282 4921.  
E-mail address: [mhkoike@hq.jnc.go.jp](mailto:mhkoike@hq.jnc.go.jp)

As for the theory, Thiruvengadam [4] derived an equation for the threshold criterion for erosion. Springer [5] proposed an equation which represented the incubation time for erosion from liquid droplets. However, these investigations were performed almost exclusively on erosion–corrosion of materials under single-phase flows. In respect of erosion–corrosion under water vapour two-phase flows, few erosion–corrosion experiments and erosion–corrosion theories have been reported. Koike [6] performed erosion–corrosion experiments for stainless steel pipes under water vapour two-phase flow conditions with steam quality of 15%. This paper describes erosion–corrosion experimental results for straight and curved pipes of stainless steel using a large loop, under water vapour two-phase flow conditions with steam quality of 26%.

## 2. Experimental procedure

Erosion–corrosion experiments were performed by the use of a CTL, in which high-temperature, pressurized, two-phase water vapour is circulated. Fig. 1 shows the schematic flow diagram of the CTL. Maximum pressure and temperature capabilities of the CTL are 8.1 MPa and 297 °C, respectively. Maximum water flow rate and steam flow rate are 120 t/h and 15 t/h, respectively. A boiler supplies heat to water and circulation pumps pressurize the water in the CTL. Water vapour two-phase flow is produced by mixing hot water and steam. After they are mixed, the two-phase water vapour flows into the erosion–corrosion test sections, then to a direct condenser which separates vapour from the two-phase flow. Vapour is circulated by a steam compressor at high speed. There are three test channels in the CTL, but only one is shown in the figure.

Four types of erosion–corrosion test sections were made in order to achieve four different flow speeds by varying the pipe diameter of each test section. Many small, straight- and curved-pipe specimens cut in round slices (about 15 mm length, 5 mm thick) were lined in series and fixed in four erosion–corrosion test sections of the CTL, as shown in Fig. 1. These inner diameters are 73.7, 62.1, 49.4 and 38.3 mm (JIS pipes). The pipe specimens were inserted into ceramics liners to avoid electrochemical corrosion of the specimens, and the specimens lined-up in series were also inserted into the pipe (straight-pipes and 350 mm radius elbow-pipes) and fixed. Specimen weight was measured before and after the erosion–corrosion test. The two-phase water vapour was flowed from a test section of large inner diameter, that is, from a test section of 73.7 mm diameter to others of 62.1, 49.4 and 38.3 mm diameter, in order. The two-phase flow rate was constant during the experiments, so that the velocity of the flow increased as the diameter of the test section became smaller. The erosion–corrosion experiment with four different velocities was performed as a constant flow rate test.

In order to estimate thickness loss by erosion–corrosion for the outlet pipes of the power stations under two-phase water vapour flow conditions, pipe-type specimens rather than plate-type specimens must be used for the experiments, because the two-phase flow pattern is very complicated compared with single-phase flow pattern and plate-type specimens are not appropriate for simulating the conditions experienced by the outlet pipes. The two-phase flow pattern of the present experiments were classified as annular mist flow type (classified by mass flow rate and steam quality), as shown in Fig. 2 [7].

Table 1 shows the chemical composition of the material used for specimens in the present work. Type 316L

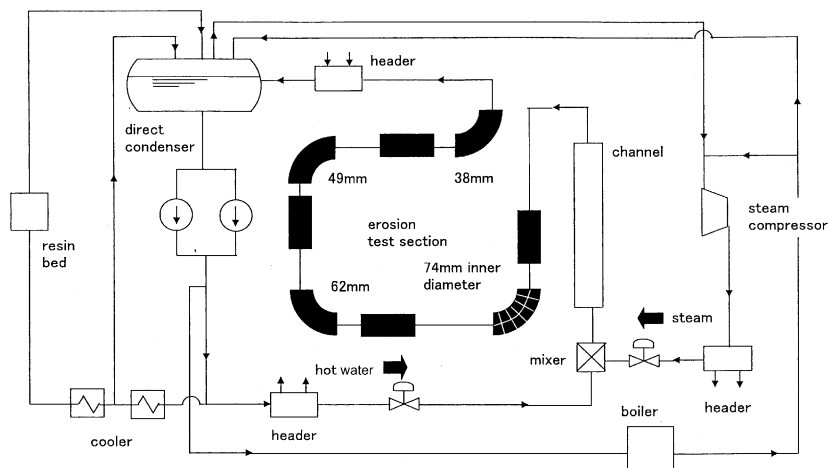


Fig. 1. Flow diagram of component test loop.

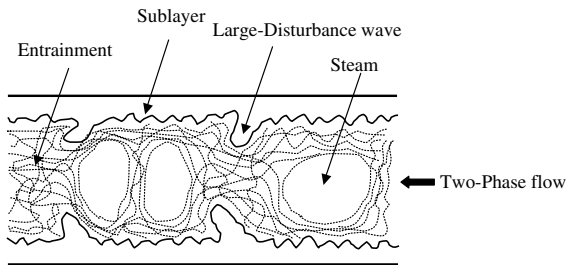


Fig. 2. Schematic diagram of annular mist two-phase flow.

stainless steel has less sensitivity to stress corrosion cracking because of its low carbon constitution, and is used in nuclear power stations.

The erosion–corrosion experimental conditions were as follows:

steam quality (steam wt%): 26% (steam 6.9 t/h, water 18.9 t/h)  
 experimental period:  
 straight-pipes: 898, 1158, 2057 h  
 curved-pipes: 2057 h  
 temperature and pressure: 292 °C, 7.6 MPa  
 water chemistry: pH 9.7,  $\leq 2$  ppb DO, 11  $\mu\text{S}/\text{cm}$  (all volatile treatment: AVT)  
 steam velocities of two-phase flow: 14, 20, 32 and 53 m/s.

The erosion–corrosion loss of the test specimens was estimated from the specimen weight difference before and after erosion–corrosion tests. The erosion–corrosion loss ( $\Delta W$ ) is expressed as

$$\Delta W = W_1 - W_0, \quad (1)$$

where  $W_0$  is the initial specimen weight before test, and  $W_1$  is the post-test specimen weight after removal of the test oxide film on the specimen by chemical reagents. The chemical reagents used here removed the oxide film only and did not attack the base metal, which was examined using blank test. Two kinds of reagents were used for the film removal, one alkali permanganate, the other citric-oxalic acid with inhibitor.

The flow speeds of the water vapour two-phase flow were calculated by the use of quality ( $x$ ) and void fraction ( $\alpha$ ). For instance, the true vapour speed ( $V_G$ ) of two-phase flow is expressed as

$$V_G = \frac{xW}{\alpha A \gamma_G}, \quad (2)$$

where  $W$ ,  $A$  and  $\gamma_G$  are total two-phase flow rate, the cross section area of pipe and the density of vapour, respectively. Void fraction was obtained from the equations of Bankoff and Jones [8].

After testing, the inner surfaces of the specimens were examined by a scanning electron microscope (SEM) to detect the severity of erosion–corrosion attack. Analyses using auger electron spectroscopy (AES) were performed on the oxide films on the specimen surfaces, especially for oxygen level. By etching the oxide films up to the base metal using argon ions, fractions of elements which comprise the films were obtained quantitatively. Also, X-ray diffraction analyses were performed on the films to determine the types of oxides formed.

### 3. Results and discussion

Experimental results obtained by the use of straight- and curved-pipe (elbow type) test sections are described here.

Figs. 3 and 4 shows the experimental data for straight-pipe and curved-pipe tests, respectively. The steam quality was 26%, and the very low dissolved oxygen (DO) level ( $\leq 2$  ppb) resulting from the use of AVT water treatment produced the least-corrosive condition for materials. Fig. 5 shows the relationship between erosion–corrosion loss and testing time for straight-pipe tests.

All of the data are summarized in Table 2, in which the erosion losses of type 316L stainless steel are represented by the unit of reduced thickness per year,  $\mu\text{m}/\text{year}$ . In the Table,  $V_L$  and  $V_{GL}$  are the water velocities of the two-phase flow and the average velocity of the two-phase flow, respectively.

By the use of SEM, examination was performed on the specimen inner surfaces after the tests. Oxide films covered all the surface of the specimens, and in several places oxide films were observed to be peeled off by erosion–corrosion. However, the degree of erosion attack was not very severe, because the depths of the peeled-off places were shallow.

Chemical profiles through the thickness of the oxide films were made by the use of AES, with etching of successive layers of film by argon-gas ion bombardment. Fig. 6 shows a typical AES spectrum of a specimen surface. The abscissa corresponds to etching time, which corresponds to depth from the film surface, and the ordinate corresponds to the atomic percentages of elements. For the

Table 1  
Chemical composition of test material, type 316L stainless steel (wt%)

Element	Fe	Cr	Ni	C	Mo	Mn	Si	P	S
Wt%	68.29	16.26	12.14	0.015	2.03	0.79	0.43	0.032	0.012

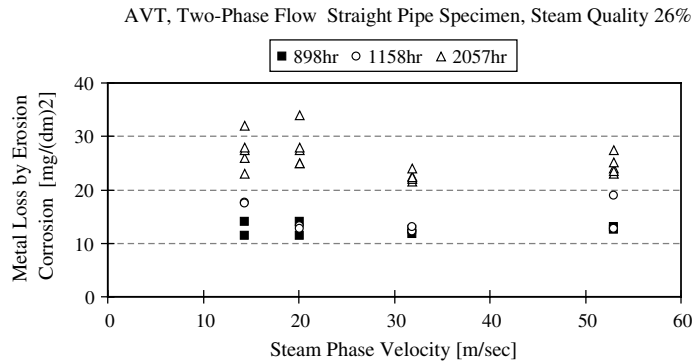


Fig. 3. Experimental results of erosion corrosion tests for straight pipe specimens.

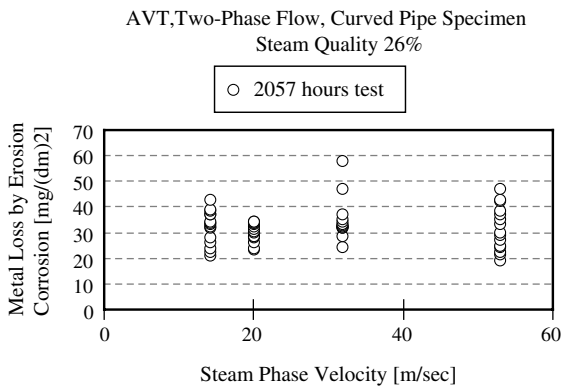
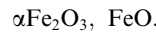


Fig. 4. Experimental results of erosion corrosion tests for curved pipe specimens.

straight-pipe specimens, the thickness of the films and the oxygen content of the films were 1–1.5  $\mu\text{m}$  and 8–10 wt%, respectively after 2057 hours of test. For the curved specimens, 0.6–2.4  $\mu\text{m}$  and 4–11 wt%, respectively.

Moreover, X-ray diffraction analyses were performed on the erosion–corrosion specimens to determine the

chemical formulae of the oxide films. By the analyses, the oxide films were determined to consist mainly of the following oxides:



After the erosion–corrosion tests, the oxide films of specimen surface were removed by reagents in order to measure the specimen weight ( $W_1$ ) of Eq. (1). The weight differences were obtained between before and after the film removal. From these data and the AES analyses, the density of oxide films was found to be 1  $\text{g}/\text{cm}^3$ . This value is much smaller than that of base metal.

As shown in Figs. 3 and 5 for straight-pipe tests, erosion–corrosion losses of type 316L stainless steel did not increase with increasing steam phase flow velocity over the range of 14–53 m/s. For single-phase flow, like water, erosion losses typically are directly dependent on the flow velocity, that is, erosion loss increases with increasing flow velocity. For the case of two-phase flow in the present study, the flow pattern of the water–vapour two-phase flow plays an important role for erosion. The flow pattern of the two-phase flow in this work was classified as annular mist flow type in which the liquid phase consists of a sublayer, with a large distur-

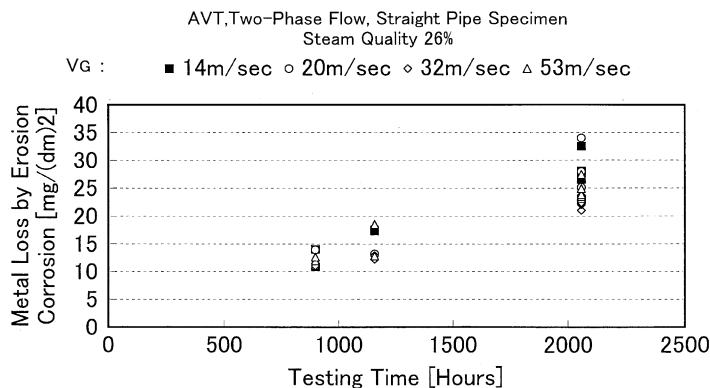


Fig. 5. Relation between erosion corrosion loss and testing time for straight pipe specimens.

Table 2

Experimental results of erosion corrosion tests under water–vapour two-phase flow conditions<sup>a</sup>

$V_G$ (m/s)	14.3	20.1	31.9	53
$V_L$ (m/s)	6.8	9.5	15.1	25.1
$V_{GL}$ (m/s)	7.9	11	17.5	29.1
Straight pipe specimen thickness loss ( $\mu\text{m}/\text{year}$ )				
898 h	$1.5 \pm 0.1$	$1.5 \pm 0.2$	$1.5 \pm 0.1$	$1.5 \pm 0.1$
1158 h	$1.6 \pm 0.1$	$1.2 \pm 0.1$	$1.2 \pm 0.1$	$1.5 \pm 0.3$
2057 h	$1.5 \pm 0.2$	$1.5 \pm 0.2$	$1.2 \pm 0.1$	$1.3 \pm 0.1$
Curved pipe specimen thickness loss ( $\mu\text{m}/\text{year}$ )				
2057 h	$1.7 \pm 0.3$	$1.6 \pm 0.2$	$1.9 \pm 0.4$	$1.7 \pm 0.4$

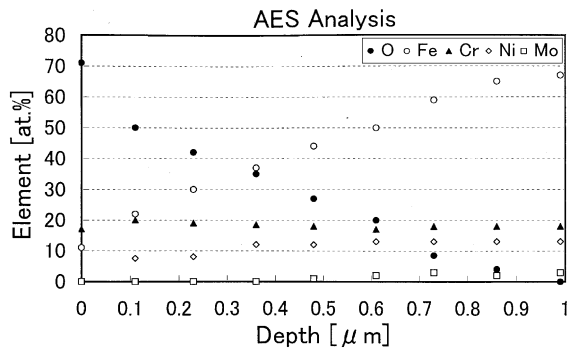
 $V_G$ : steam velocity  $V_L$ : water velocity  $V_{GL}$ : two-phase velocity.<sup>a</sup> AVT: pH 9.7, DO  $\leq 2$  ppb, 11  $\mu\text{S}/\text{cm}$ , quality 26%, 292 °C, 7.6 MPa, Steam 6.9 t/h, Water 18.9 t/h.

Fig. 6. AES analysis of specimen inner surface.

bance wave streaming on the sublayer at higher speed, causing entrainment, and steam flows along center of the pipe [8]. For the present test, erosion–corrosion loss of materials results from by both erosion and corrosion, in which erosion is caused by the flow patterns, and corrosion is caused mainly by dissolved oxygen in the flow ( $\leq 2$  ppb, which is considered very small). In Fig. 2, the large-disturbance liquid waves (LD waves) proceed smoothly on sublayer flows. The speed of the LD waves is one order higher than that of the sublayer [9], so that the attack of LD waves on the pipe surfaces is considered to be weak. Entrainment occurs near the top of the LD waves by the action of accelerated steam flow. The erosion–corrosion loss of the straight-pipe is considered to result mainly to sublayer kinetic energy, not from LD waves. When the flow speed of two-phase flow increases, the thickness of sublayer flow decreases [9]; conversely, when the flow speed of two-phase flow decreases, the thickness of sublayer flow increases. As a result, the kinetic energy of the sublayer flow is probably very similar for both cases. Actually, erosion–corrosion losses in the straight-pipe tests were found to be almost constant for various flow velocities.

For the curved-pipe (elbow type) tests, sublayers, LD waves, entrainments, and steam were mixed. Erosion–corrosion losses result from the attack of the mixed

flows, and the water chemistry (e.g. dissolved oxygen). The erosion–corrosion losses in the present study were in the range of 1.6–1.9  $\mu\text{m}/\text{year}$  (2057 h test), which is slightly larger than that for the straight pipe (1.2–1.6  $\mu\text{m}/\text{year}$ ). Under AVT water treatment, the dissolved oxygen was very low ( $\leq 2$  ppb), so that the attack by the mixed flows was also considered to be small.

#### 4. Conclusion

(1) Erosion–corrosion experiments on type 316L stainless steel under water vapour two-phase flow were performed by the use of a component test loop for the outlet pipes of reactors and boilers. Experiments were performed for straight-pipes and curved-pipes (350 mm radius elbow), with test conditions of AVT ( $\leq 2$  ppb DO, pH 9.7, steam quality 26%), in which steam velocities of the two-phase flow were studied in the range of 14–53 m/s. Results of the erosion–corrosion loss were as follows:

Straight-pipe tests: 1.2–1.6  $\mu\text{m}/\text{year}$ ;

Curved-pipe tests: 1.6–1.9  $\mu\text{m}/\text{year}$ .

Values of the erosion–corrosion loss are very small for the both straight-pipes and curved-pipes, and almost constant over the range of steam phase velocities of 14–53 m/s.

(2) Analyses of the oxide films on specimen surfaces gave the following information:

1. The oxide films were determined by X-ray diffraction analyses to be mainly  $\alpha\text{Fe}_2\text{O}_3$  and FeO;
2. Quantitative elemental depth profiles of the oxide films were determined by AES analyses, in which oxygen and metallic elements were quantitatively obtained in the oxide films. The thickness of the films, and oxygen content in the films, were 1–1.5  $\mu\text{m}$  and 8–10 wt% for the straight-pipe tests, respectively, and 0.6–2.4  $\mu\text{m}$  and 4–11 wt% for the curved-pipe tests, respectively;

3. The densities of oxide films were calculated to be  $1 \text{ g/cm}^3$ .

#### **Acknowledgement**

The authors wish to thank Ryowa Industry Co., Ltd. for their earnest and safe operation of component test loop during the erosion–corrosion tests.

#### **References**

- [1] G. Ito, Y. Shimizu, S. Sato, *Corros. Eng.* 18 (8) (1969) 9 (in Japanese).
- [2] Y. Okada, A. Iwamoto, K. Sano, *Trans. JSME* 43 (1977) 8 (in Japanese).
- [3] C.F. Palomero, E. Hifrensa, K. Garbett, in: *Proceedings of the Water Chemistry 3*, BNES, London, 1983, p. 235.
- [4] A. Thiruvengadam, *ASTM STP* 408 (1966) 22.
- [5] G.S. Springer, *Erosion by Liquid Impact*, John Wiley & Sons, 1976.
- [6] M.H. Koike, H. Baba, *Proceedings of 1988 JAIF International Conference on Water Chemistry in Nuclear Power Plants*, Tokyo, 2, 532.
- [7] K. Akagawa, *Two Phase Flow*, Corona, Tokyo, 1976 (in Japanese).
- [8] S.G. Bankoff, *Trans. ASME, Ser. C* 82 (1960) 35.
- [9] K. Sekoguchi, K. Nishikata, M. Nakatomi, H. Nishi, A. Kaneuji, *Trans. JSME* 39 (317) (1973) 313 (in Japanese).